Characterization and Liquid Chromatography–MS/MS Based Quantification of Hydroxylated Fullerenes

ARTICLE *in* ANALYTICAL CHEMISTRY · FEBRUARY 2011

Impact Factor: 5.64 · DOI: 10.1021/ac1031379 · Source: PubMed

6 AUTHORS, INCLUDING:

Tzu-Chiao Chao
University of Regina
31 PUBLICATIONS **698** CITATIONS
SEE PROFILE

Guixue Song
Pony Test International
13 PUBLICATIONS **368** CITATIONS
SEE PROFILE

Nicole Hansmeier
Universität Osnabrück
24 PUBLICATIONS **394** CITATIONS
SEE PROFILE

Paul Westerhoff
Arizona State University
221 PUBLICATIONS **10,394** CITATIONS
SEE PROFILE

Published in final edited form as:
Anal Chem. 2011 March 1; 83(5): 1777–1783. doi:10.1021/ac1031379.

Characterization and LC-MS/MS based quantification of hydroxylated fullerenes

Tzu-Chiao Chao[1,2,3,>], **Guixue Song**[1,>], **Nicole Hansmeier**[3], **Paul Westerhoff**[1], **Pierre Herckes**[2], and **Rolf U. Halden**[1,3,*]

[1]School of Sustainable Engineering and The Built Environment, Arizona State University, Tempe, AZ 85287, United States

[2]Department of Chemistry and Biochemistry, Arizona State University, Tempe, AZ 85287, United States

[3]The Biodesign Institute at Arizona State University, Center for Environmental Biotechnology, Tempe, AZ 85287, United States

Abstract

Highly water-soluble hydroxylated fullerene derivatives are being investigated for a wide range of commercial products as well as for potential cytotoxicity. However, no analytical methods are currently available for their quantification at sub-ppm concentrations in environmental matrices. Here, we report on the development and comparison of liquid chromatography-ultra violet/visible spectroscopy (LC-UV/vis) and mass spectrometry (LC-MS) based detection and quantification methods for a commercial fullerols. We achieved good separation efficiency using an amide-type hydrophilic interaction liquid chromatography (HILIC) column (plate number >2000) under isocratic conditions with 90% acetonitrile as the mobile phase. The method detection limits (MDLs) ranged from 42.8 ng/mL (UV detection) to 0.19 pg/mL (using MS with multiple reaction monitoring, MRM). Other MS measurement modes achieved MDLs of 125 pg/mL (single quad scan, Q1) and 1.5 pg/mL (multiple ion monitoring, MI). Each detection method exhibited a good linear response over several orders of magnitude. Moreover, we tested the robustness of these methods in the presence of Suvanee River fulvic acids (SRFA) as an example of organic matter commonly found in environmental water samples. While SRFA significantly interfered with UV- and Q1-based quantifications, the interference was relatively low using MI or MRM (relative error in presence of SRFA: 8.6% and 2.5%, respectively). This first report of a robust MS-based quantification method for modified fullerenes dissolved in water suggests the feasibility of implementing MS techniques more broadly for identification and quantification of fullerols and other water-soluble fullerene derivatives in environmental samples.

Keywords

Nanomaterial; Mass Spectrometry; MRM; Hydrophilic Interaction Chromatography; HILIC; MALDI-TOF; Hydroxylated Fullerenes; Fullerenols; Fullerols

[*]Corresponding Author. Rolf U. Halden, Center for Environmental Biotechnology, The Biodesign Institute at Arizona State University, 1001 S. McAllister Avenue, P. O. Box 875701, Tempe, AZ, 85287, USA. halden@asu.edu; Fax: +1 (480) 727-0889; Tel: +1 (480) 727-0893.
[>]Both Authors Contributed Equally

Supporting information is available free of charge at http://pubs.acs.org

Introduction

Carbonaceous nanomaterials are projected to have a tremendous impact in the biomedical field.1 One particular vision is to engineer nanomaterials that can carry a payload of drugs and other clinically relevant compounds to a target delivery site, *e.g.*, to cancer cells.2 Fullerenes are especially attractive due to their stability and the wide range of possible modifications. Hydroxylated fullerenes (also called fullerenols or fullerols) were among the first synthesized water-soluble C_{60} derivatives.3 This functionalization can change the solubility of these compounds from less than 10^{-9} mg/L for C_{60} to >50 mg/L for fullerols.4, 5 Higher derivatized C_{60} fullerols with a solubility of 6 g/L also have been reported.6 These fullerols are under investigation for use in biomedical applications, due to their antioxidant abilities and also are in development as drug carriers for their ability to bypass protective bodily interfaces, including the blood-retina and the blood-brain barriers.7–12 Using different modifications, water-solubilized fullerenes were also found to possess antioxidative, antibacterial, and antiviral properties, thereby opening up a wide range of possible applications.13–18 In addition, fullerol films are under investigation for possible use in the conversion of solar energy. 19

Various methods have been developed to synthesize water-soluble fullerols. These include the hydrolysis of a fullerene intermediate through the use of, *e.g.*, nitronium chemistry20, sulfuric and nitric acid21, 22, 6, and nitrogen dioxide radicals23. Alkaline approaches have been intensively studied and utilize the reaction of NaOH with fullerene assisted by different catalysts, such as tetrabutylammonium hydroxide (TBAH)3, polyethylene glycol (PEG) 400 24, and H_2O_2 5, 25. At least one commercial fullerol manufacturer uses alkaline hydrolysis of $C_{60}Br_{24}$.26 Fullerols synthesized by the above methods typically represent complex mixtures, and commercially available fullerols are therefore not chemically pure.27

These medicinal and industrial uses of fullerols are expected to increase in the future, resulting in their occurrence in environmental samples and biological fluids. The high bioavailability of fullerols, their potential for bioaccumulation, and their ability to generate reactive oxygen species after photoactivation have raised concerns about potential adverse effects on humans and the environment.28–33 Although several studies have demonstrated relatively low toxicity of fullerols in comparison with fullerenes, there is still no firm consensus regarding their health risks.34, 35 Moreover, quantitative data on the occurrence of fullerols are currently lacking, owing to the dearth of available quantification methods. In this report, we characterize a commonly used commercial fullerol and describe different liquid chromatography tandem mass spectrometry (LC-MS/MS) approaches for its detection and quantification in aqueous samples. The sensitivity, accuracy, and dynamic range of these different methods are compared and their value assessed for the analysis of environmental water samples containing natural organic matter.

Experimental Methods

Chemicals

The fullerol salt $[C_{60}(OH)_x(ONa)_y$, which has a composition of $x+y=24$ with y generally around 6–8] was purchased from Materials and Electrochemical Research Corporation and had an indicated purity of >95% (MER, Tucson, AZ, USA). Fullerol stock solutions were prepared by mixing 1.3 mg of fullerol powder in 2 mL of LC grade water. The fullerol stock was vortexed for 10 min or sonicated for 20 min, filtered through a 0.2 μm nylon syringe filter, and stored in a brown glass vial at 4°C. Acetonitrile, water, ammonium hydroxide, acetic acid and formic acid were obtained at LC-MS grade (Sigma Aldrich, St. Louis, MO, USA). Suwanee River fulvic acids (SRFA) were obtained from the International Humic

Substances society (http://ihss.gatech.edu/), lot number 1S101F, as a representative environmental dissolved organic matter.

Characterization with TEM, DLS and FTIR

Transmission electron microscopy (TEM) and dynamic light scattering (DLS) were used to determine the size distribution of the generated fullerol suspension. A Philips CM200-FEG TEM/STEM was operated at 200 kV to obtain high resolution TEM images of the aqueous fullerol solution. A copper grid with lacey-carbon support film was brought in contact with a 50-μl drop of the fullerol stock solution and air dried before imaging. In order to assess the colloidal stability, the zeta potential and hydrodynamic diameter of the nanoparticles (or aggregates of nanoparticles) were measured using the ZetaPals 90Plus analyzer (Brookhaven Instruments Corp, Holtsville, NY, USA). The samples were filtered through a 0.45-μm nylon filter prior to analysis. The zeta potential was measured as a function of pH to investigate the effect of pH on the potential of fullerol solutions. Briefly, 10 mL of fullerol solution (3.8 mg/mL) was prepared in 0.1 M KNO_3 solution. The fullerol solution was titrated to the desired pH value using 0.1 M or 0.01 M HNO_3. Then, the zeta potential of the suspension was measured immediately. Six runs per measurement were acquired for each sample.

Fourier transform infrared (FTIR) spectra were obtained on freeze-dried samples as KBr pellets using a Bruker IFS 66V/S FTIR spectrometer scanning from 4,000 to 400 cm^{-1} and averaging 64 scans at 1.0-cm^{-1} intervals with a resolution of 4.0 cm^{-1}.

MALDI-TOF-MS

An ABI 4800 matrix-assisted laser desorption/ionization (MALDI) time-of-flight (TOF) mass spectrometer (Applied Biosystems, Framingham, MA, USA) was used to obtain spectra of fullerenes and fullerols. The fullerenes were dispersed in toluene, whereas fullerols were vortexed in water. A total of 1 μl of each sample was spotted on a steel target or mixed with different matrices (alpha-cyano-4-hydroxycinnamic acid, sinapinic acid, and 2,5-dihydroxybenzoic acid) directly on the target. After air drying, mass spectra from the samples were obtained in positive and negative mode by taking 1000 shots each. The signal was generally higher in the absence of a matrix.

LC-MS(/MS) and LC-UV/Vis

Mass spectrometric analyses were carried out on an API 4000 instrument (Applied Biosystems, Framingham, MA, USA), coupled to a Shimadzu Prominence HPLC (Shimadzu Scientific Instruments, Inc., Columbia, MD, USA). The system was controlled by Analyst 1.5 software (Applied Biosystems, Framingham, MA, USA). Separation was carried out using a Waters XBridge C_{18} (3.5 μm, 4.6 × 100 mm) or an XBridge amide column (3.5 μm, 4.6×150 mm, Waters Chromatography, Milford, MA, USA). Liquid chromatography was carried out under isocratic conditions at a flow of 0.5 mL/min. For the C_{18} column, concentrations between 10% and 90% (v/v) acetonitrile in water were tested in 10% increments, whereas for the amide columns acetonitrile concentrations between 50% and 90% were used. In addition, the effects of additives such as acetic acid, ammonium hydroxide, and formic acid at concentrations of 0.1 – 1% (v/v) on separation efficiency and signal strength were also investigated. A Shimadzu SIL-20AC autosampler was used for injection of 10-μl aliquots of the fullerol samples.

The signal was much higher in positive mode, and optimized ionization conditions were obtained with the following settings: curtain gas, collision gas, nebulizer gas, and heater gas at 11, 7, 60, and 30 psi, respectively; temperature at 300°C; and ion spray (IS) voltage at 4500 V. Compound-dependent parameters were as follows: declustering potential of 115 V,

entrance potential of 10 V, collision energy of 120 V, And collision exit potential of 9 V. The precursor masses used for multiple ion (MI) scanning and multiple reaction monitoring (MRM) analyses were set to the following *m/z* ratios: 1129, 1055, 981, 907, 833, 759, 685, 611, 537, and 520. A thorough cleaning process between runs was necessary to reduce fullerol contamination of the LC-MS system. LC-UV/Vis analyses were carried out using a Waters 2695 HPLC system (Waters, Milford, MA) equipped with a UV/Vis detector (Waters module 2996) using the same columns and LC conditions as described above for the LC-MS system. The only modification was a larger sample injection volume (50 μl). Method detection limits (MDLs) were determined by calculating the standard deviation of at least seven injections and multiplying the obtained value with the one-sided critical-*t* level at the 99% confidence level. The plate number was calculated with $N=5.54\left(\frac{t_m}{W_{0.5}}\right)^2$, with t_m being the migration time and $W_{0.5}$ the half maximal width.36

Results and Discussion

Characterization of MER fullerol

Despite their common use, few data that characterize commercial C_{60} fullerols in aqueous solutions are available. This is problematic because their properties may differ significantly from source to source or even between batches. It is therefore useful to establish the basic properties of the material as a reference prior to the development of a new detection and quantification method. Thus, we employed several standard analytical techniques to assess characteristics of a commonly used commercial fullerol sodium salt with the empirical formula $C_{60}(OH)_x(ONa)_y$, where the sum of *x* and *y* equaled 24 and *y* ranged from 6 to 8. In the following, this material is referred to as MER fullerol.

TEM images of single MER fullerol cores and larger aggregates in water are shown in Figures 1a and 1b, respectively. The core cluster has a diameter of approximately 19 nm and may be formed by hydrogen bonding (C-OH and C-O^-) among individual fullerol molecules.6 In solution the size distributions (Figure 1c) of sonicated fullerol samples were relatively polydispersed (polydispersity index of 0.314) with a maximum peak at approximately 45 nm. Without sonication the particle size was much larger, with a maximum of 200–350 nm (not shown).

The zeta potential is an index of the magnitude of interaction between colloidal particles and is therefore routinely used to assess the stability of colloidal systems. Due to the high hydroxylation state of fullerols strong pH dependency was expected. In fact, above pH 6 the zeta potential of an aqueous MER fullerol solution was −15 to −25 mV (Figure 1d), indicating moderate stability. At pH values ranging from 3 to 6 the potential was less negative (−5 to −10 mV) which coincides with reduced colloidal stability.

Thus the fullerol was stable at higher pH due to the presence of neutral and partially ionized (C-O^-) fullerol molecules present in solution. With decreasing pH, the zeta potential of protonated fullerol particles increased, and the fullerol aggregates became more and more unstable and started to precipitate when the pH was close to the isoelectric point. We found that the fullerol precipitated at approximately pH 1.8, which is consistent with the reported isoelectric point of 1.7 for $C_{60}(OH)_{18}$ fullerol.37

The FTIR spectrum of fullerol is presented in Figure 2. This sample displayed a broad OH-stretching band at approximately 3429 cm^{-1}, C-O stretching at 1066 cm^{-1}, C-O-H bending at 1364 cm^{-1}, and C=C stretching at 1634 cm^{-1}. These four bands have been reported as diagnostic absorptions of various fullerols.20, 6, 5 However, this commercial fullerol also showed additional peaks that had been reported previously. These included a peak at 1453

cm^{-1} that was ascribed to -OH bending as well as another one at approximately 841 cm^{-1} that may be assigned to C-C stretching.38 This highlights the need to properly characterize the fullerol species under investigation.

Qualitative UV/Vis spectroscopy, MALDI and ESI-MS

The methods above characterize fullerols but generally are not suited for quantification in complex environmental samples. We therefore explored the use of UV/Vis spectroscopy and mass spectrometric analyses for detection as a basis for subsequent quantification of fullerols. UV/Vis spectroscopy has been used successfully to quantify C_{60} fullerenes.39 However, the UV/Vis spectrum of fullerol is featureless compared to pristine fullerene. Figure 3 shows the water-soluble fullerol UV/Vis spectrum in ultrapure water. The fullerol exhibits broad spectra asymmetrically decreasing in absorbance into the visible light range.

We further investigated the fullerols with mass spectrometric techniques using matrix-assisted laser desorption/ionization (MALDI) and electrospray ionization mass spectrometers. Both are considered soft ionization techniques. However, since fullerenes and fullerols can absorb laser energy with high efficiency,40, 41 the resulting ionization mode could be more similar to pure laser desorption ionization (LDI). In the MALDI-MS spectra we found a major peak at *m/z* 720, which corresponds to the molecular mass of C_{60} (supplementary Figure S-1; panels a and b). In addition, a peak series from *m/z* 720 to 576 with a spacing of 24 *m/z* was found. This has also been observed in earlier studies of fullerenes and has been attributed to sequential C_2 losses.42, 43, 23

Notably, we also found an increasing peak series spaced by 24 *m/z* units starting at *m/z* 720, which suggests the addition of C_2 to the molecule. While an observed peak at *m/z* 1128 could in theory correspond to a completely hydroxylated fullerol $[C_{60}(OH)_{24}]^+$, the consistency of the series as well as the fact that the series extends beyond the expected maximum mass of 1304 for $[C_{60}(ONa)_8(OH)_{16}]^+$ suggest otherwise. For direct comparison, we also analyzed a C_{60} sample with MALDI-MS and found that at the same settings and laser intensities the C_2-cluster fragmentations and additions were much less pronounced than those of the fullerol (Figure S-1, panel c). Higher molecular weight fullerene formation by C-2 cluster additions during laser ablations is a well-known phenomenon, 44 and our data suggest that hydroxylated fullerols may be more reactive as a substrate than fullerenes. Nonetheless, the overall similarity of the fullerol and fullerene mass spectra does not allow a confident differentiation between these two types of nanomaterials using MALDI.

For fullerols ESI could be a gentler method than LDI or even MALDI and may be capable of preserving diagnostic hydroxyl moieties in the fullerol sample, thereby allowing for a distinction to be made between different fullerol and fullerene species. The ESI-MS analysis of C_{60} fullerols resulted in a complex spectrum (Figure 4) with only a weak peak corresponding to the protonated molecular mass of fullerol $[C_{60}(OH)_{24} + H]^+$ at *m/z* 1129. In contrast to the MALDI-TOF spectra, no C_2 series were found. However, a closer inspection revealed a decreasing series spaced by 74 *m/z* units from *m/z* 1129 to 537 $[M-n74+H]^+$ with n = 1–8. The mass differences could be tentatively explained by subsequent neutral losses of $C_2H_2O_3$. This could also explain the observation that the series does not continue past *m/z* 537, which would correspond to $[C_{44}H_8O+H]^+$, as only a single oxygen is left. Moreover, another strong peak was found at *m/z* 520, which could be explained by the loss of an additional hydroxyl group. As a general trend, the peak intensity decreased with increasing *m/z* ratio, and it can be speculated that higher hydroxylation promotes the observed fragmentation of the fullerol. We also found a second, slightly shorter series of 74 *m/z* units ranging from *m/z* 1073 to 703. The *m/z* difference between peaks of these two series is approximately 17–18 *m/z* units, which suggests the presence of an additional hydroxyl group in the second series. Overall, the data show that despite the instability of

fullerols, during ionization, the regular and reproducible fragmentation may be diagnostic enough to provide a stable basis for further analyses. This is in agreement with an earlier report from Isaacson et al. that mentioned the absence of ions diagnostic for fullerols during MALDI, ESI, and atmospheric pressure chemical ionization (APCI)-MS analyses.45 However, a difference in this study was the detection of a small peak corresponding to the protonated molecular ion of fullerol and the identification of a diagnostic 74-*m/z* series.

UV- and MS-based quantification

UV/Vis spectroscopy has been routinely used for the analysis of fullerenes. 45 We therefore tested, whether it may also apply to the analysis of fullerols. Because no distinct absorption peaks were observed with UV/Vis spectroscopy, we chose 254 nm to measure fullerol, as we found a low signal background at this wavelength. A linear correlation was observed between UV absorbance at 254 nm and fullerol concentration (Table 1) with an effective extinction coefficient of 5400 $\mu g L^{-1} cm^{-1}$. While this shows that UV spectroscopy can in theory be used to quantify neat fullerols, the lack of any distinct absorption peaks as well as the potential presence of interfering substances in environmental samples may severely limit its use. Similar concerns have been raised regarding UV-based quantitation of fullerenes in environmental samples.46

Our data indicated three possible routes for the mass spectrometric quantification of fullerols by ESI-triple-quadrupole analysis. First is a Q1 scan that measures across the whole range of fullerol peaks. However, due to the broad range of masses to be scanned, the method may have low sensitivity, especially in presence of interfering compounds. While this method is unsuited for accurate quantification in complex matrices, it can be used for initial screens of very pure samples, e.g. to assess decomposition products due to aging. Second, a multiple ion (MI) scan could be used that includes only the observed peaks of the 74 *m/z* series as well as the *m/z* 520 ion. However, the highest sensitivity and specificity could be reached using multiple reaction monitoring (MRM) during which the same ions would be fragmented and diagnostic fragmentation products would be monitored. To achieve this, we generated fragmentation spectra of MER fullerol. Using high collision energies, we were able to obtain reproducible fragmentation spectra (Figure S-2) from all selected ions. In all analyses a peak at *m/z* 73 was detected and tentatively assigned to $[C_6 + H]^+$, which we used as a diagnostic transition for MS/MS-based analyses of fullerols.

LC-MS for fullerol separation and quantification

To allow quantification of fullerols in complex samples, a separation process is necessary prior to MS or UV/Vis analysis. Several HPLC methods exist for the separation and quantification of fullerenes using hydrophobic column materials (*e.g.*, C_{18}).45 However, the retention mechanism cannot be classified as reverse-phase separation because the solvents as well as stationary phase are nonpolar for fullerene separations.47 Reverse-phase separation has found application in the separation of some water-soluble fullerenes, for example dendrofullerenes.48 The stronger hydroxylation of the MER fullerol and the associated negative surface charges may interfere with reverse phase separation approaches. A possible solution is the use of amide phase hydrophilic interaction chromatography (HILIC) column, which provides positive surface charges. Thus, we tested and compared the efficiency of a C_{18} column with an, HILIC amide column for C_{60} fullerol separation.

To compare separation efficiency with the two columns and different solvents, we used an HPLC coupled to a triple-quadrupole mass spectrometer and monitored the fullerol peak by scanning the mass range of *m/z* 520–1150. The separation was conducted under isocratic conditions with different ratios of acetonitrile/water or methanol/water as mobile phases. In addition, we tested the effect of different additives (see methods section) and calculated

plate numbers as a measure of separation efficiency. With a C_{18} column, we were unable to reach a satisfying retention of the analyte regardless of the mobile phase composition and additives used. Accordingly, the calculated plate number did not exceed 34. Apparently, the hydroxyl groups inhibited the interaction of the fullerene core with the stationary phase.

In contrast, the HILIC amide column, which provides negative surface charges, resulted in a theoretical plate number of approximately 2264 ± 141, thus indicating efficient retention when using 90% acetonitrile as the mobile phase. While the addition of NH_4OH increased the plate number to approximately 3400, it also strongly reduced the peak intensity (data not shown). The retention time showed good reproducibility (RSD = 0.4%).

Overall, the data suggest that a suitable detection method consists of a chromatographic separation with an amide HILIC column and subsequent detection and quantification using a non-discriminative Q1 or Q3 scan, an MI scan, or MRM. Generally, overview scans using a single quadrupole are of limited sensitivity and specificity. However, the observation that fullerols are prone to fragmentation represents an important finding of this study.

Detection limits

We proceeded to test and validate the above methods with the analysis of a dilution series of neat fullerols. Samples were separated through the HILIC amide column followed by quantification using a UV detector (at 254 nm) or ESI-MS in one of the three scan modes. Using UV detection, the MDL was 42.8 ng/mL. The MDLs of ESI-MS-based measurements were highly dependent on the scan mode, which strongly affects the signal-to-noise ratio (S/N). Overall, the S/N of the peak signals increased from Q1 to MI scan to MRM. For example, using a 60 pg/mL MER fullerol stock solution, the S/N increased from 14.5 with the Q1 scan to 976.8 with the MRM scan (Figure 5). Accordingly, we found the highest MDL with a Q1 scan (0.125 ng/mL), followed by the MI scan (1.5 pg/mL), and finally an MRM scan (0.19 pg/mL; Table 1). The detection limit of the MRM analysis therefore corresponded to the total injection of a minimum of approximately 140,000 fullerol molecules. An earlier report on ESI-MS-based detection of unmodified fullerenes achieved a detection limit of 0.02 ng/mL,49 which is comparable to the MDL obtained by us with MI scans for MER fullerols.

All methods yielded an excellent linear response (R^2 ranged between 0.999 and 0.9999) over a broad dynamic range as determined by a serial dilutions starting from the respective MDL up to 800 ng/mL for the MS-based methods and up to 5 μg/mL for the UV-based detection. The reproducibility of the MS-based methods was assessed by repeated measurements over a period of four weeks and was found to be similarly low for MRM and MI scans (RSDs of 0.5 and 0.7%, respectively) and higher for the Q1 analysis (RSD of 2.9%; Table 1)

It thus appears that the MRM mode may be most appropriate for the testing of environmental samples, especially as the monitoring of transitions reduces quantification errors that can result from the presence of compounds with similar masses. To test this and to simulate the presence of dissolved organic matter in environmental water samples, we spiked dilute fullerol standards (1 ng/mL) to a >1000-fold excess (2.5 μg/mL final concentration) with Suwanee River fulvic acid (SRFA). As seen in Table 1, we found the lowest relative error in the presence of SRFA when using MRM transitions as compared to a Q1 or MI scan. The relatively low error (2.5%) for MRM indicates that this method might be useful for the detection of fullerols in the environment. Quantification of fullerols with UV/Vis was not possible in the presence of SRFA, as the SRFA and fullerol signals were indistinguishable (data not shown).

To further validate the methods, we measured pure SRFA samples (2.5 μg/mL) with the same parameters. Scanning with Q1 yielded a small peak at the retention time for fullerol with a peak area corresponding to ~3 ng/mL fullerol. This indicates that Q1 measurements are not specific enough to differentiate between fullerols and organic matter extant in natural waters. In contrast, MI and MRM scans of SRFA samples did not yield detectable peaks (not shown).

Conclusions

Overall, our results demonstrate that LC-MS/MS-based approaches for the detection and quantification of fullerols are feasible and that the MRM approach may be best suited for analysis of water samples at the highest attainable specificity. Sufficient chromatographic separation was obtained using an amide-based HILIC column, which performed better than the reverse-phase columns generally used for fullerene analyses. This is the first report of a robust MS-based quantification method for modified fullerenes dissolved in water. Its success suggests the feasibility of implementing MS techniques for identification and quantification of fullerols and other water-soluble fullerene derivatives in environmental samples.

Supplementary Material

Refer to Web version on PubMed Central for supplementary material.

Acknowledgments

Guixue Song and Tzu-Chiao Chao contributed equally to this work. The project described here was supported in part by Award Number 1RC2ES018801 and R01ES015445 from the National Institute of Environmental Health Sciences (NIEHS). The content is solely the responsibility of the authors and does not necessarily represent the official views of the NIEHS or the National Institutes of Health.

References

1. Martin CR, Kohli P. Nat. Rev. Drug. Discov. 2003; 2:29–37. [PubMed: 12509757]
2. Ferrari M. Nat. Rev. Cancer. 2005; 5:161–171. [PubMed: 15738981]
3. Li J, Takeuchi A, Ozawa M, Li X, Saigo K, Kitazawa K. J. Chem. Soc. Chem. Commun. 1993:1784–1785.
4. Ruoff R, Malhotra R, Huests D, Tse D, Lorents D. Nature. 1993; 362:140–141.
5. Kokubo K, Matsubayashi K, Tategaki H, Takada H, Oshima T. ACS NANO. 2008; 2:327–333. [PubMed: 19206634]
6. Vileno B, Marcoux P, Lekka M, Sienkiewicz A, Feher T, Forro L. Adv. Funct. Mater. 2006; 16:120–128.
7. Chaudhuri P, Paraskar A, Soni S, Mashelkar R, Sengupta S. ACS NANO. 2009; 3:2505–2514. [PubMed: 19681636]
8. Partha R, Conyers J. Int. J. Nanomed. 2009; 4:261–275.
9. Ji Z, Sun H, Wang H, Xie Q, Liu Y, Wang Z. J. Nanopart. Res. 2006; 8:53–63.
10. Cai X, Jia H, Liu Z, Hou B, Luo C, Feng Z, Li W, Liu J. J. Neurosci. Res. 2008; 86:3622–3634. [PubMed: 18709653]
11. Saitoh Y, Xiao L, Mizuno H, Kato S, Aoshima H, Taira H, Kokubo K, Miwa N. Free Radic. Res. 2010; 44:1072–1081. [PubMed: 20815770]
12. Torres VM, Srdjenovic B, Jacevic V, Simic VD, Djordjevic A, Simplício AL. Pharmacol. Rep. 2010; 62:707–718. [PubMed: 20885011]
13. Lee J, Mackeyev Y, Cho M, Li D, Kim J, Wilson L, Alvarez P. Environ. Sci. Technol. 2009; 43:6604–6610. [PubMed: 19764224]

14. Li Q, Mahendra S, Lyon D, Brunet L, Liga M, Li D, Alvarez P. Water Res. 2008; 42:4591–4602. [PubMed: 18804836]
15. Brunet L, Lyon D, Hotze E, Alvarez P, Wiesner M. Environ. Sci. Technol. 2009; 43:4355–4360. [PubMed: 19603646]
16. Srdjenovic B, Milic-Torres V, Grujic N, Stankov K, Djordjevic A, Vasovic V. Toxicol. Mech. Method. 2010; 20:298–305.
17. Piotrovsky L, Kiselev O. Fuller. Nanotub. Car. N. 2004; 12:397–403.
18. Djordjevic A, Canadanovic-Brunet J, Vojinovic-Miloradov M, Bogdanovic G. Oxid. Commun. 2004; 27:806–812.
19. Kleiman-Shwarsctein A, Jaramillo T, Baeck S, Sushchikh M, McFarland E. J. Electrochem. Soc. 2006; 153:C483–C487.
20. Chiang L, Upsani R, Siwrczweski J. JACS. 1992; 114:10154–10157.
21. Chiang L, Wang L, Swirczewski J, Soled S, Cameron S. J. Org. Chem. 1994; 59:3960–3968.
22. Chiang L, Upsani R, Swirczewski J, Soled S. JACS. 1993; 115:5453–5457.
23. Chiang L, Bhonsle J, Wang L, Shu S, Chang T, Hwu J. Tetrahedron. 1996; 52:4963–4972.
24. Zhang J, Yang W, He P, Zhu S. Chinese J. Chem. 2004; 22:1008–1011.
25. Wang S, He P, Zhang J, Jiang H, Zhu S. Synthetic Commun. 2005; 35:1803–1808.
26. Djordjevic A, Vojinovic-Miloradiv M, Petranovic P, Devecerski A, Bogdanovic G, Adamov J. Arch. Oncol. 1997; 5:139–141.
27. Troshin P, Astakhova A, Lyubovskaya R. Fuller. Nanotub. Car. N. 2005; 13:331–343.
28. Roberts J, Wielgus A, Boyes W, Andley U, Chignell C. Toxicol. Appl. Pharm. 2008; 228:49–58.
29. Yamago S, Tokuyama H, Nakamura E, Kikuchi K, Kananishi S, Sueki K, Nakahara H, Enomoto S, Ambe F. Chemistry & Biology. 1995; 2:385–389. [PubMed: 9383440]
30. Brunet L, Lyon DY, Hotze EM, Alvarez PJJ, Wiesner MR. Environ. Sci. Technol. 2009; 43:4355–4360. [PubMed: 19603646]
31. Pickering KD, Wiesner MR. Environ. Sci. Technol. 2005; 39:1359–1365. [PubMed: 15787378]
32. Zhao B, He Y, Bilski PJ, Chignell CF. Chem. Res. Toxicol. 2008; 21:1056–1063. [PubMed: 18422350]
33. Badireddy AR, Hotze EM, Chellam S, Alvarez P, Wiesner MR. Environ. Sci. Technol. 2007; 41:6627–6632. [PubMed: 17948818]
34. Zhu X, Zhu L, Li Y, Duan Z, Chen W, Alvarez P. Environ. Toxicol. Chem. 2007; 26:976–979. [PubMed: 17521145]
35. Gelderman M, Simakova O, Clogston J, Patri A, Siddiqui S, Vostal A, Simak J. Int. J. Nanomed. 2008; 3:59–68.
36. Poole, C.; Poole, S. Chromatography Today, Fifth Edition. Elsevier Science; 1991.
37. Li X, Chen Z, Guo G, Deng S. Journal of Instrumental Analysis. 2009; 48:432–435.
38. Alves GCA, Ladeira LO, Righi A, Krambrock K, Calado HAD, Gil RPDF, Pinheiro MAVB. J. Brazil. Chem. Soc. 2006; 17:1186–1190.
39. Andrievsky GV, Klochkov VK, Bordyuh AB, Dovbeshko GI. Chem. Phys. Lett. 2002; 364:8–17.
40. Ugarov MV, Egan T, Khabashesku DV, Schultz JA, Peng H, Khabashesku VN, Furutani H, Prather KS, Wang HJ, Jackson SN, Woods AS. Anal. Chem. 2004; 76:6734–6742. [PubMed: 15538798]
41. Havel J, Soto-Guerrero J. J. Radioanal. Nucl. Ch. 2005; 263:489–492.
42. O'Brien SC, Heath JR, Curl RF, Smalley RE. J. Chem. Phys. 1988; 88:220.
43. Luffer D, Schram K. Rapid Commun. Mass Spectrom. 1990; 4:552–556.
44. Creasy WR, Zimmerman JA, Ruoff RS. J. Phys. Chem. 1993; 97:973–979.
45. Isaacson CW, Kleber M, Field JA. Environ. Sci. Technol. 2009; 43:6463–6474. [PubMed: 19764203]
46. Taylor R, Abdul-Sada A. Fuller. Sci. Technol. 2000; 8:47–54.
47. Guillaume YC, Peyrin E. Anal. Chem. 1999; 71:1326–1331. [PubMed: 21662953]

48. Gharbi N, Burghardt S, Brettreich M, Herrenknecht C, Tamisier-Karolak S, Bensasson RV, Szwarc H, Hirsch A, Wilson SR, Moussa F. Anal. Chem. 2003; 75:4217–4222. [PubMed: 14632138]

49. Isaacson CW, Usenko CY, Tanguay RL, Field JA. Anal. Chem. 2007; 79:9091–9097. [PubMed: 17963360]

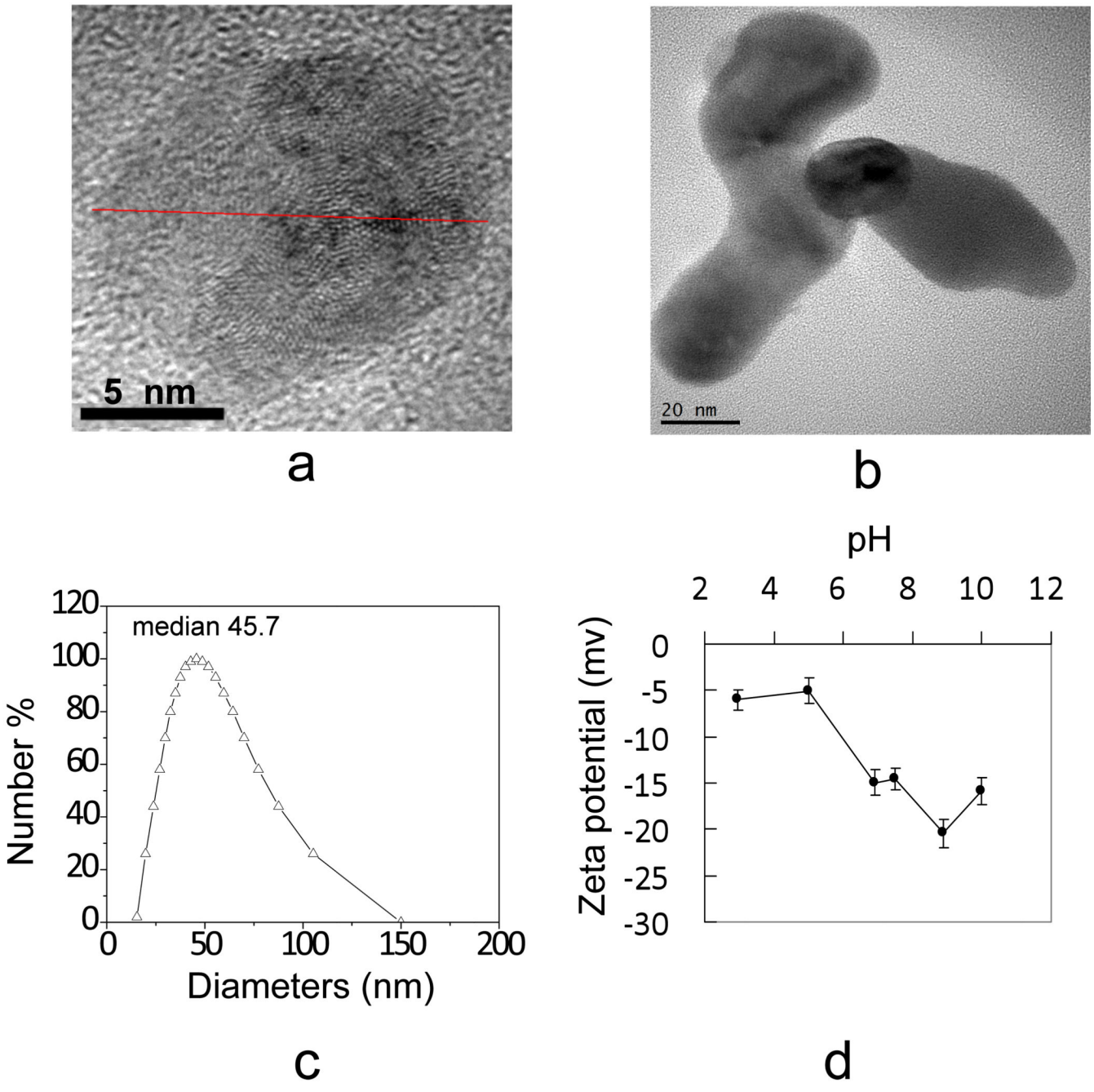

Figure 1.
Characterization of MER fullerols. Panels a and b show TEM images of smaller fullerol cores and larger aggregates, respectively. Panel c shows the size distribution of sonicated aqueous fullerol stock solution. Panel d shows the pH dependence of the zeta potential of a fullerol suspension.

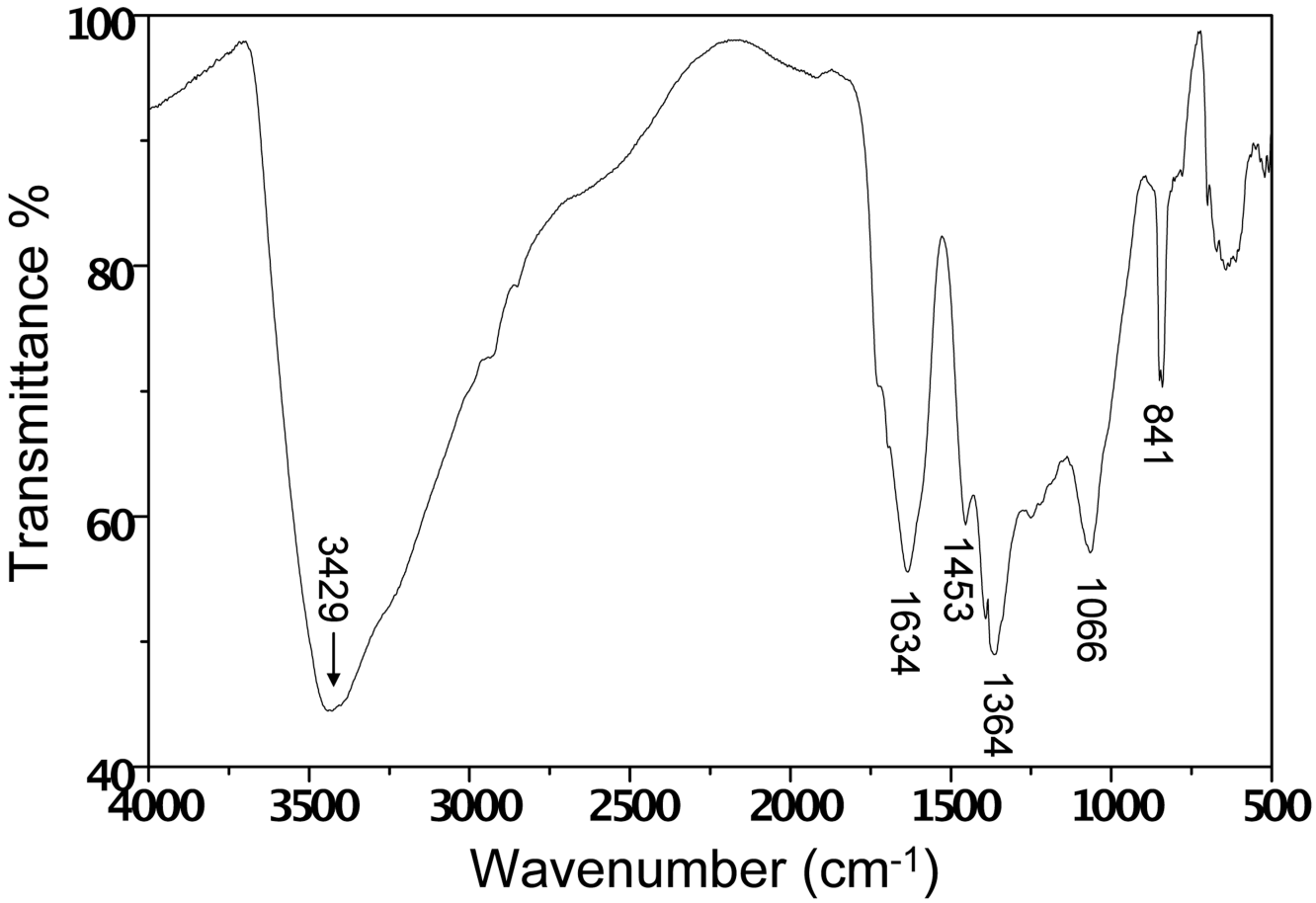

Figure 2.
FTIR spectrum of a MER fullerol sample. Details for the interpretation of the wavelength numbers are given in the main text.

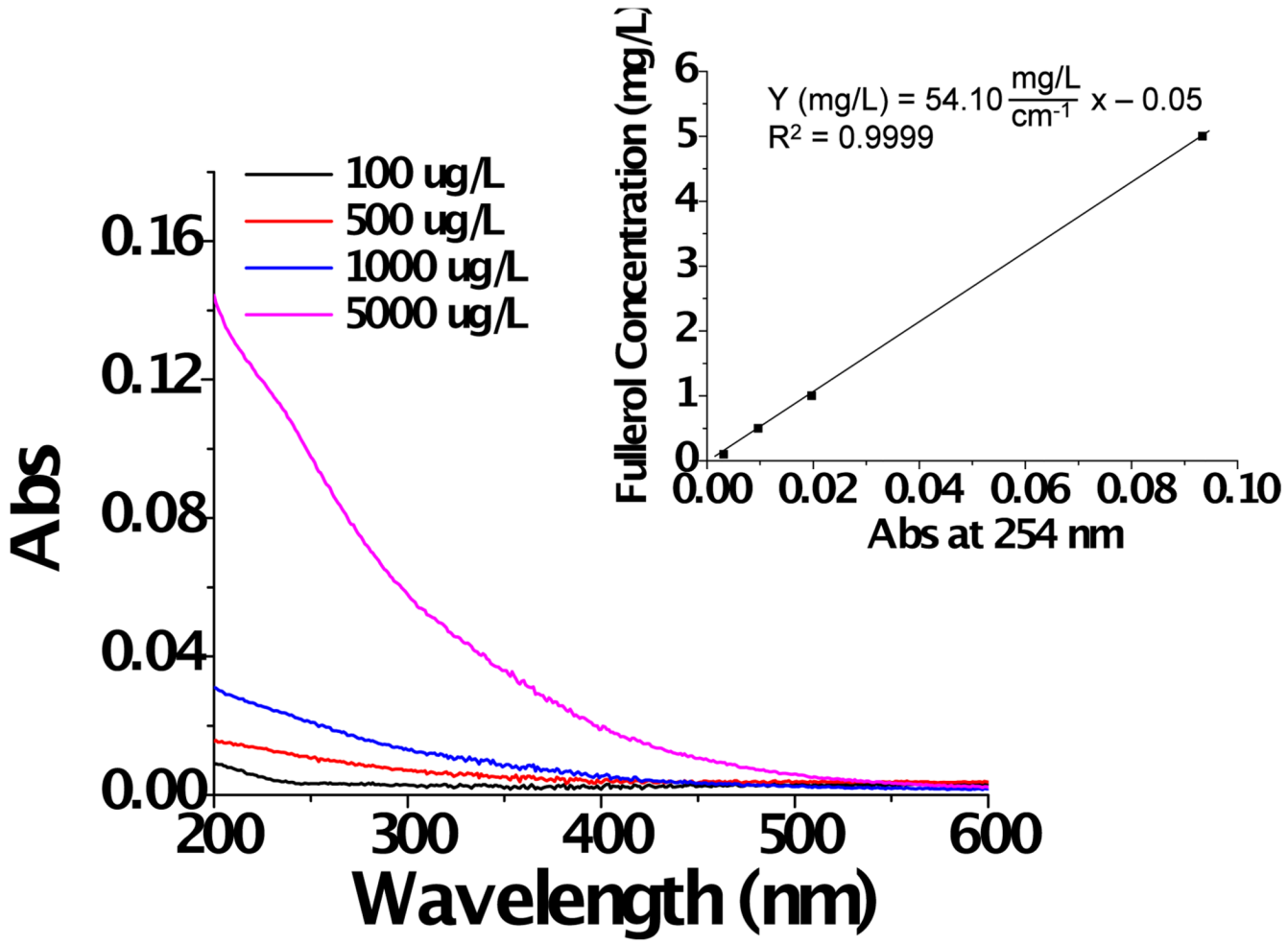

Figure 3.
UV spectroscopy of MER fullerol. The fullerol did not exhibit specific absorbance peaks. The inset shows a four-point calibration curve obtained at a wavelength of 254 nm.

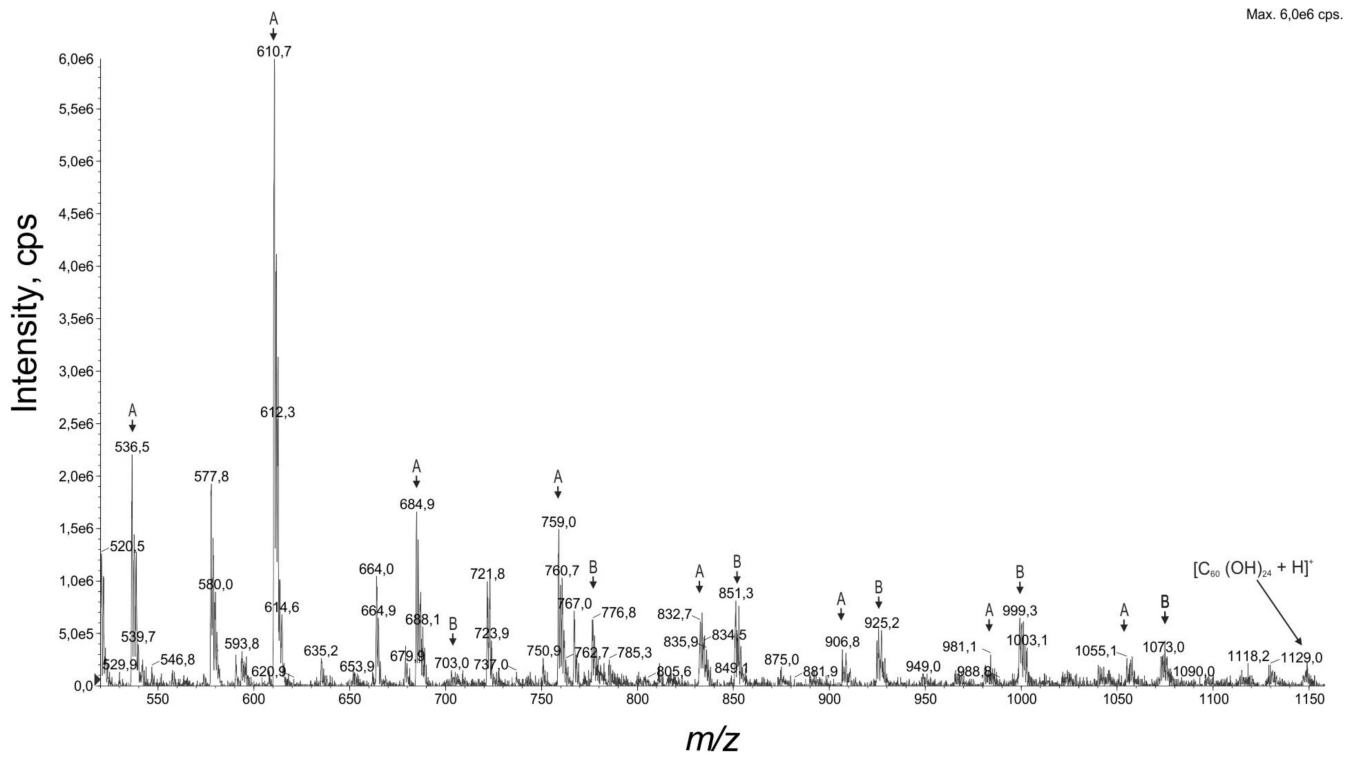

Figure 4.

Overview (Q1)-scan of a MER fullerol sample. Peaks of the two 74-*m/z* series (A and B) are indicated by the arrows.

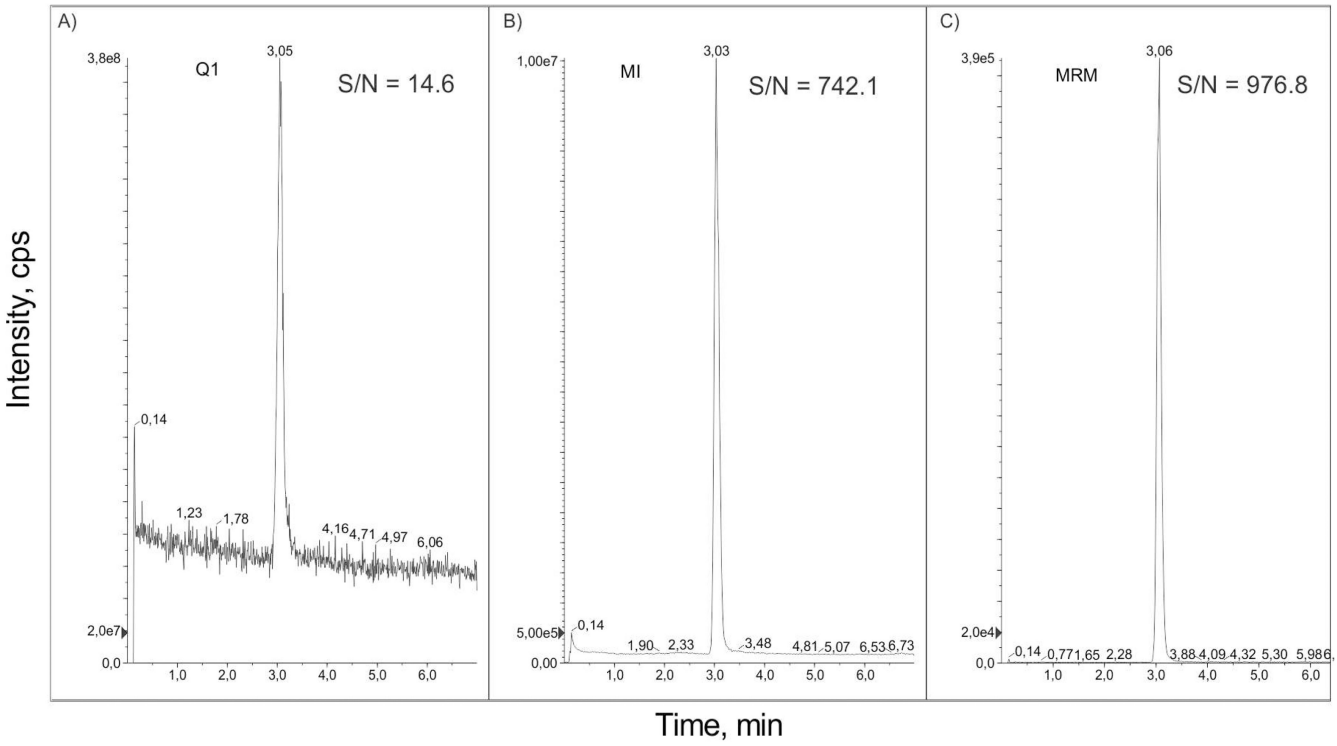

Figure 5.

Representative LCMS chromatograms of a 60 pg/mL fullerol solution using different MS scan methods. A) Q1 scan of masses between *m/z* 520 and 1150. B) Multiple ion scan using the major peaks of the 74 *m/z* series. C) MRM using the transition of the major 74 m/z series peaks to *m/z* 73. The signal-to-noise (S/N) ratios for each peak are indicated.

Table 1

Performance of HPLC with different detection methods

	R^{2a}	MDL[b] [pg/mL]	RSD[c]	SRFA[d]
UV/Vis	0.999	42 780	n.d.	n.d.
Q1 scan	0.9996	125	2.9 %	29.4 %
MI scan	0.9999	1.5	0.7%	8.6 %
MRM scan	0.9999	0.19	0.5 %	2.5 %

a) Eight-point calibration from the respective MDL to 800 ng/mL (MS) or four-point calibration 100 ng/mLto 5 μg/mL (UV)

b) Concentration of standard, 10 μl injection (MS) or 50 μl injection (UV)

c) Relative standard deviation resulting from measurement of standard at 45 ng/mL during a four-week period (n=16)

d) Relative error from a standard at 10 ng/mL spiked with 2.5 μg/mL Suwanee River fulvic acids (SRFA; n=8)